Regioselectivity of Michael Additions to 3-(Pyridin-3-yl or Pyrimidin-2-yl)-propenoates and Their *N*-Oxides – Experimental and Theoretical Studies

Elzbieta Lewandowska*[a] and David C. Chatfield*[b]

Keywords: Michael addition / Regioselectivity / Substituent effects / Density functional calculations

We demonstrate that nucleophilic addition to α,β-unsaturated carbonyl compounds can be redirected from the usual β-carbon (Michael) to an α-carbon regioselectivity by attaching a π-deficient aromatic substituent to the β-carbon atom. In particular, propanethiol addition to 3-(pyridin-3-yl or pyrimidin-2-yl)propenoate gives a β-carbon adduct, while addition to the corresponding more π-deficient *N*-oxides gives the α-adduct or a mixture of α- and β-adducts. This adds to the number of carbon–carbon bond-forming reactions at the α-position of Michael receptors documented recently. Density functional calculations reveal that the regioselectivity is due to a combination of reduction of the barrier for α-addition and increase of the barriers for β-addition and carbonyl addition as the π-deficient character of the aromatic substituent is increased. The calculations predict a significant solvent effect on the regioselectivity in some cases. The regioselectivity is also consistent with Hammett constants σ^-.

Introduction

The Michael reaction is one of the most fundamental approaches for the formation of new carbon–carbon and carbon–heteroatom bonds.[1] Among the manifold carbon–carbon bond-forming reactions, the Michael addition is especially valuable for creating a new bond selectively at the β-position of activated olefins. Recently, reverse addition of nucleophiles to α,β-unsaturated carbonyl compounds has been reported.[2,3] Trost et al.[4] and Yamamoto et al.[5] have developed new methods for constructing a new carbon–carbon bond at the α-position of Michael acceptors by palladium-catalyzed complexes. Phosphane-catalyzed nucleophilic addition at the α-position of alkynoates has also been reported by Trost et al.[6] and Liu et al.[7] An analogous regioselectivity has been reported for the Michael addition of thiols to fumaric derivatives[8,9] and of organolithium reagents to cinnamic acids.[10,11]

We recently reported studies on the regioselectivity of the Michael addition of the cyanide anion (theoretical model) and propanethiolate nucleophile (experimental studies) to various α,β-unsaturated aldehydes and esters possessing different electron-withdrawing substituents at the β-carbon atom.[12] We found that two nitro groups or one nitro and one trifluoromethyl group in the phenyl ring attached to the β-carbon atom reverses the polarity of the carbon–carbon double bond and redirects the regioselectivity of nucleophilic addition from the usually observed β- to an abnormal α-addition. We have shown that appropriate electron-withdrawing groups (EWGs) can be chosen to effect the desired nucleophilic addition at either the α- or the β-carbon atom in an α,β-unsaturated carbonyl compound. We have also shown that the regioselectivity of Michael addition can be predicted from partial atomic charges and properties of the frontier orbitals of the reactants.

We now report experimental and theoretical results on several Michael addition reactions of propanethiol with propenoate esters having a pyridin-3-yl or pyrimidin-2-yl ring attached to the β-carbon atom. We find that a 1-oxopyridin-3-yl moiety makes α- and β-addition almost equally favorable, and a 1-oxopyrimidin-2-yl moiety favors α-addition. Hammett constants and density functional theory (DFT) calculations are generally consistent with these results and provide a basis for prediction and interpretation. In particular, the Hammett constants σ^- are correlated with the experimental regioselectivity and with the calculated transition state energies for α-addition.

[a] University of Agriculture,
60-625 Poznan, Poland
Fax: +48-61-8487824
E-mail: elalew@au.poznan.pl
[b] Florida International University,
Miami, FL 33199, USA
Fax: +01-305-348-3772
E-mail: David.Chatfield@fiu.edu
Supporting information for this article is available on the WWW under http://www.eurjoc.org or from the author.

Results and Discussion

Experiment

The starting propenoate esters **2** and **9** were obtained by condensation of the appropriate 3-pyridinecarbaldedyde (**1**) and 2-pyrimidinecarbaldehyde (**8**) (obtained in situ by reduction of methyl pyrimidine-2-carboxylate with DIBAL

at –70 °C in hexane solution) with the stabilized ethoxycarbonylmethylene Wittig reagents. Treatment of ethyl 3-(pyridin-3-yl)propenoate (**2**) with propanethiol in the presence of EtONa/EtOH produced β-addition product **4** in 73% yield (Scheme 1). Oxidation of **2** with *meta*-chloroperoxybenzoic acid gave the corresponding *N*-oxide **3**, which has an even stronger electron-withdrawing effect. Reaction of **3** with propanethiol gave a mixture of β- and α-adducts **5** and **6** in a 1:2 ratio (estimated by ^{1}H NMR spectrum). In order to increase the α-regioselectivity, the propenoate ester **9** with the more π-deficient pyrimidin-2-yl ring attached to the β-carbon atom was prepared. Surprisingly, treatment of ethyl 3-(pyrimidin-2-yl)propenoate (**9**) with propanethiol also gave exclusively the β-addition product **11** (Scheme 2). However, the corresponding *N*-oxide, upon treatment with propanethiol, produced the α-adduct. The structures of α- and β-adducts were confirmed by 2D NMR spectroscopy and high-resolution mass spectrometry. Thus, β-adducts **4**, **5**, and **11** have diastereotopic CH_2 protons with signals at δ = 2.92, 3.20; 2.96, 3.12; and 2.96, 3.20 ppm. The α-adducts **6** and **12** show these proton signals shifted downfield at δ = 3.26, 3.42 and 3.51, 3.70 ppm. On the other hand, the CH proton signal is observed at δ = 4.36, 4.99 and 4.45 ppm for β-adducts **4**, **5**, and **11**, but it is shifted upfield to δ = 4.22 and 4.00 ppm in the case of the α-adducts **6** and **12**.

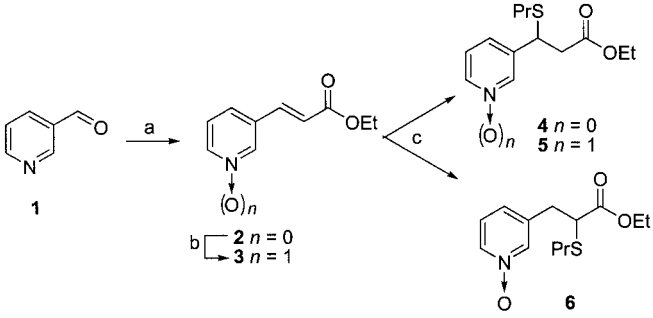

Scheme 1. Synthesis of pyridinyl compounds. Reagents: (a) Ph_3P=$CHCO_2Et$/MeCN; (b) *m*CPBA/CH_2Cl_2; (c) PrSH/EtOH/EtONa.

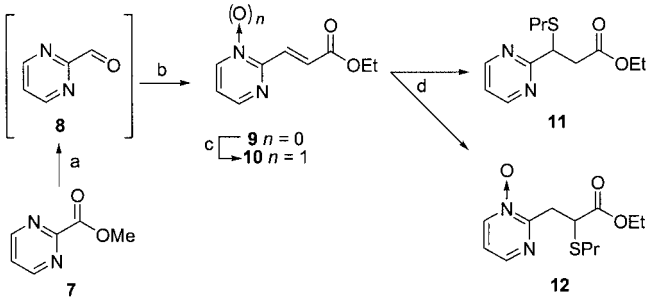

Scheme 2. Synthesis of pyrimidinyl compounds. Reagents: (a) DIBAL/hexane/CH_2Cl_2; (b) Ph_3P=$CHCO_2Et$; (c) *m*CPBA/CH_2Cl_2; (d) PrSH/EtOH/EtONa.

Computation

Calculations at the DFT (B3LYP) and MP2 levels (see Computational Methods) were performed for attack of cyanide anion on each of compounds **2**, **3**, **9**, and **10** at three sites: The α-carbon atom (C_α), the β-carbon atom (C_β), and the carbonyl carbon atom (C_c). Cyanide anion was chosen as the nucleophile to complement previous calculations we had performed on related molecules.[12] Additional calculations were performed for compounds **3** and **9** using methanethiolate as the nucleophile. The regioselectivities for the two nucleophiles appear to be quite similar.

Table 1 gives transition-state energies $E^\ddagger_\alpha$, $E^\ddagger_\beta$, and $E^\ddagger_c$ for the nucleophilic addition step of α-, β-, and carbonyl addition, respectively, relative to the energies of van der Waals complexes. The same van der Waals complex was used as the reference for all nucleophilic additions to a given compound (see Computational Methods). Also given in Table 1 are the Hammett constants σ^-. Protonation of the enolate intermediate is probably very fast and is not considered here.[13] Examples of transition states are shown in Figure 1 for α-, β-, and carbonyl addition to **2**. The general expectation was that increasing the electron deficiency of the aromatic ring, correlated here with σ^-, would improve the favorability of α-addition with respect to β-addition. This can be understood classically as a stabilization of resonance structure (c) relative to (b) in Figure 2. The experimentally observed change from β- to α-addition (**2, 9** → **3** → **10**) is in fact correlated with increasing σ^-. It is also correlated with decreasing $E^\ddagger_\alpha$ and increasing $E^\ddagger_\beta$ and $E^\ddagger_c$. The excellent correlation between σ^- and $E^\ddagger_\alpha$ (Figure 3) is not unexpected, since σ^- reflects the stability of a negative charge at the carbon atom adjacent to a phenyl ring, such as possessed by the intermediate of α-addition. Carbonyl addition is never favored, consistent with experiment. While calculation and experiment are in clear agreement for **2** and **10**, the predictions for **3** and **9** are the reverse of experiment. However, the difference between the transition-state energies $E^\ddagger_\alpha$ and $E^\ddagger_\beta$ is small (< 3 kcal/mol) in these cases, close to the computational uncertainty for the method and consistent with the finding that the α- and β-additions are competitive for **3**. In fact, the transition states for α-, β-, and carbonyl addition are within 5 kcal/mol in all cases, suggesting that circumstances might be chosen (solvent, sub-

Table 1. Hammett constants[a] (σ^-) and transition-state energies[b] [kcal/mol] for α-, β-, and carbonyl addition.

Compound	σ^-	$E^\ddagger_\alpha$[c]	$E^\ddagger_\beta$[c]	$E^\ddagger_c$[c]
2	0.76	17.9	13.0	14.9
3	2.25	15.2	12.6	15.1
9	1.98	15.9	17.3	17.9
10	3.47	14.0	19.0	19.5

[a] The values of σ^- are asterisked entries designated C5H4N1@, 3-pyridyl, S.META- (**2**); C5H4N1@, 3-pyridyl *N*-oxide, S.META- (**3**); and C4H3N2@, 2-pyrimidinyl, S.ORTH- (**9**) in *Exploring QSAR*.[27] No experimental value for **10** could be found, so additivity was assumed and σ^- was taken as the value for **9** plus the difference between the values for **3** and **2**, i.e., it was assumed that attaching an oxygen atom to a nitrogen atom has the same effect on **9** (leading to **10**) as on **2** (leading to **3**). [b] B3LYP/6-31+G(d), gas phase. [c] Transition-state energies $E^\ddagger$ are relative to the same van der Waals complex for all additions to a given compound.

stituents, nucleophile) to favor any of the three or mixtures of them.

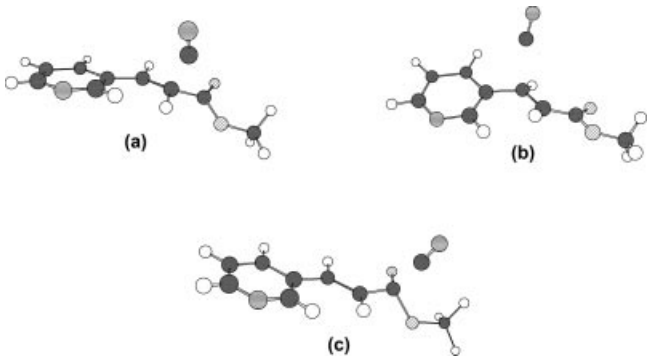

Figure 1. Transition states for (a) α-, (b) β-, and (c) carbonyl addition of cyanide anion to **2**. Selected interatomic distances are given in Table 2. Element patterns: carbon = solid; hydrogen = white; nitrogen = horizontal lines; oxygen = diagonal lines; sulfur = mottled (see Figure 4).

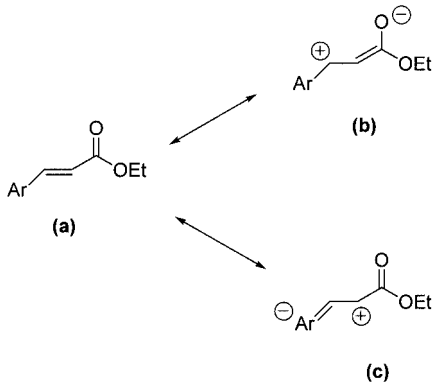

Figure 2. Propenoate resonance structures.

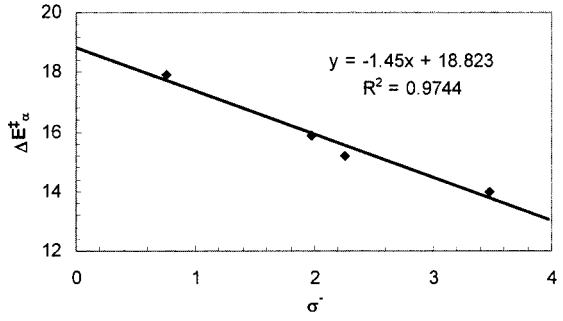

Figure 3. Transition-state energy barrier for α-addition ($\Delta E^{\ddagger}_{\alpha}$) vs. Hammett constant σ^{-}.

Inclusion of vibrational and rotational contributions to the free energy does not change this picture. Table 2 compares the transition states on the basis of $\Delta G^{\ddagger}$ (298 K, gas phase; B3LYP), defined by Equation (1), where $G^{\ddagger}$ pertains to the transition state under consideration, and the β-addition transition state is the reference.

Table 2. Transition-state free energies relative to β-transition states (298 K, kcal/mol, gas phase); see Equation (1).

Compound	$\Delta G^{\ddagger}$ [B3LYP[a]]			$\Delta G^{\ddagger}$ [MP2[b]]		
	TS_{α}	TS_{β}	TS_{c}	TS_{α}	TS_{β}	TS_{c}
2	4.95	0.00	1.94	3.10	0.00	–0.82
3	2.83	0.00	3.72	1.88	0.00	1.57
9	–1.16	0.00	0.84	–0.13	0.00	–0.95
10	–4.97	0.00	0.03	–2.47	0.00	–0.62

[a] B3LYP/6-31+G(d). [b] From MP2//B3LYP/6-31+G(d) energies and B3LYP/6-31+G(d) frequencies.

$$\Delta G^{\ddagger} = G^{\ddagger} - G^{\ddagger}_{\beta} \quad (1)$$

MP2 values are given for comparison. The general trends with respect to α- and β-attack reproduce the B3LYP results, although the magnitudes are smaller. Curiously, carbonyl attack is barely favored in three instances, but this is probably an artefact since MP2 transition-state energies are generally less accurate than B3LYP values.[14]

Lengths of the incipient carbon–carbon bonds, r_{c-c}, are given for all transition states in Table 3. These increase with decreasing transition-state energy, in agreement with the Hammond postulate.[15] Note the equivalence of r_{c-c} for the α- and β-transition states for **9**, consistent with the very small difference in transition-state energies. Additional factors underlying regioselectivity are summarized in Table 4. Partial atomic charges, calculated with the ChelpG method,[16] and contributions to the LUMO for C_{α}, C_{β}, and C_{c} of the reactant compound are given. The latter are represented by the absolute value of the coefficient of the $2p_z$ orbital ($|2p_z|$) centered on the carbon atom under consideration (the molecules lie in the *x*,*y* plane so that attack occurs in the *z*-direction). Charges increase for C_{α} and decrease for C_{β} in the sequence **2** → **3** → **9**, consistent with the regioselectivity predicted from transition state energies. However, the trend in these charges is reversed for **9** → **10**, whereas transition-state energies and experiment both find **10** to most favor α-addition. Furthermore, the carbonyl carbon atom has the largest charge, yet it is not the favored site of attack. Thus, there is not a clear correlation between the charges and the regioselectivity. On the other hand, the LUMO contributions are clearly correlated with $\Delta G^{\ddagger}$. In every case, the carbon atom with the largest $|2p_z|$ has the smallest $\Delta G^{\ddagger}$. Thus, the reaction appears to be under frontier-orbital control,[17] as we have found previously for Michael addition reactions of related compounds.[12]

Table 3. Length [Å] of incipient C–C bond (r_{c-c}) in transition-state structures.

Compound	TS_{α}	TS_{β}	TS_{c}
2	1.91	2.10	1.94
3	1.98	2.11	1.94
9	2.06	2.06	1.92
10	2.18	2.03	1.91

We further investigated whether the source of the discrepancy between the computed values of $\Delta G^{\ddagger}$ for **3** and **9** and the observed regioselectivity could be a solvation effect.

Table 4. Absolute value of coefficient of $2p_z$ orbital ($|2p_z|$) in LUMO and ChelpG charges (Q) for the three possible sites of nucleophilic attack (C_α, C_β, C_c).

Compound	$\|2p_z\|$			Q		
	C_α	C_β	C_c	C_α	C_β	C_c
2	0.26	0.29	0.22	–0.41	–0.00	0.87
3	0.27	0.28	0.21	–0.36	–0.05	0.86
9	0.27	0.24	0.19	–0.22	–0.28	0.84
10	0.27	0.22	0.17	–0.23	–0.19	0.82

We calculated solvation free energies, ΔG_{solv}, for all of the transition states, without reoptimizing, using the PCM continuum solvent method[18,19] (vide infra). When $\Delta G^\ddagger$ is corrected for ΔG_{solv}, carbonyl addition is predicted for **2** and **10**, while β-addition is predicted for **3** and **9**. This incorrect prediction probably reflects inadequacy of a continuum solvent representation for describing systems capable of hydrogen bonding. Therefore as a brief test, we added a single water molecule to the α- and β-transition state structures for **3** and **9** and reoptimized in the gas phase, keeping the nucleophilic attack distance r_{c-c} constant. For **3**, we placed the water so as to form a hydrogen bond with the oxygen atom of the dative bond, while for **9** the hydrogen bond was with a ring nitrogen atom. For **3**, the single water molecule stabilized the α-transition state relative to the β-transition state and reduced $\Delta G^\ddagger$ from 2.83 to 1.79 kcal/mol. For **9**, relative stabilization of the β-transition state was observed ($\Delta G^\ddagger$ was increased from –1.16 to 0.37 kcal/mol), due in part to formation of a second hydrogen bond, with the cyanide ion. This demonstrates that hydrogen bonding may affect the regioselectivity when other factors are in close balance. We caution against over interpretation of these results based on a single solvent molecule, however. An extensive conformational search with an explicit first solvent shell would be needed for a conclusive computational study.

Finally, in order to assess whether conclusions based on the cyanide anion are also representative of an alkyl thiolate, we performed a few calculations using methanethiolate as the nucleophile. We focused on **3** and **9** since these appear to be the sensitive cases for regioselectivity. The results are summarized in Table 5. The nonlinearity of methanethiolate requires a more extensive conformational search than for the cyanide anion. For nucleophilic attack at C_α or C_β, geometry optimizations were initiated for each of the three conformations staggered about the C_S–S–C_α–C_β or C_S–S–C_β–C_α dihedral angle, respectively. Conformations 1, 2, and 3 correspond to α-attack; 4, 5, and 6 correspond to β-attack. Conformations 1, 2, 4, and 5 are gauche relative to the C_α–C_β bond prior to optimization; 3 and 6 are *anti*.

The S–C_α or S–C_β bond length was initially set to 1.90 Å and a constrained optimization was performed, followed by a full optimization. The energies in Table 5 are relative to the lowest-energy unconstrained conformation. For **3**, all of the optimizations with constrained S–C_α bonds of length 1.90 Å resulted in higher energies than those with constrained S–C_β bonds, consistent with β-addition. The reverse was true for **9**. Thus, the energies of the constrained structures suggest a similar regioselectivity for methanethiolate and cyanide anion addition.

Table 5. Energies [kcal/mol] and conformational data for structures related to methanethiolate attack on **3** and **9**.

Reactant	Bond[a]	Initial Conformation	Constrained[a] E[b]	Constrained[a] Φ[c]	Unconstrained E	Unconstrained R_{sc}[c]	Unconstrained Φ
3	S–C_α	1	6.9	–43	0.0	2.73	–12
		2	8.5	59	0.0	2.73	–12
		3	9.5	159	2.8	2.85	142
	S–C_β	4	5.2	–50	0.2	2.64	17
		5	3.2	49	0.2	2.64	17
		6	4.3	176	4.2	1.93	176
9	S–C_α	1	3.5	–47	0.0	2.66	–8
		2	4.1	62	3.9	1.98	58
		3	5.7	–178	5.7	1.91	–178
	S–C_β	4	7.1	–38	1.4	2.73	2
		5	7.4	67	1.4	2.73	2
		6	9.0	166	3.7	2.88	163

[a] All calculations were begun with an initial bond length of 1.90 Å between the sulfur atom and C_α (for α-attack) or C_β (for β-attack). In the constrained optimizations, this distance was not allowed to change. The final geometry from the constrained optimizations was used as the input for the corresponding unconstrained optimizations. [b] All energies, both constrained and unconstrained, are relative to the lowest-energy unconstrained conformation for a given reactant. [c] Dihedral angles Φ [°] are the C_S–S–C_α–C_β and C_S–S–C_β–C_α angle for α- and β-attack, respectively. Distances r_{S-C} are the S–C_α and S–C_β distances for α- and β-attack, respectively.

The S–C_α or S–C_β distances of the fully optimized structures fall into two ranges: 1.91–1.98 Å, which corresponds to an almost fully formed S–C bond (the S–C bond length within the methanethiolate is 1.82 Å), and 2.64–2.88 Å, which is a nonbonding distance and thus represents a van der Waals complex. Surprisingly, the lowest-energy structure is a van der Waals complex for both **3** and **9**, and so in the few cases in which the strained S–C bond survived optimization (conformations 6 for **3**, and 2 and 3 for **9**), it is marginally stable.

In all cases but one (reactant **9**, conformation 2), the gauche conformations optimize to a van der Waals complex in which the methanethiolate is nearly parallel to the C_α–C_β bond, the sulfur atom approximately 2.7 Å from one carbon and one of the methyl hydrogen atoms approximately 2.5 Å from the other (e. g. Figure 4a). The interaction is partly dipole–dipole; the methanethiolate induces an increase in the partial atomic charge at the carbon atom close to the sulfur atom and susceptible to nucleophilic attack, and a decrease in the charge at the other carbon atom, where a negative charge would become localized upon attack. For example, in the van der Waals complex for **3**, conformation 1, the C_α and C_β charges change by +0.26 and –0.37 charge units, respectively, vs. isolated **3** (ChelpG charges).

Upon optimization, the *anti* conformations either retain the S–C_α or S–C_β bond (reactant **3**, conformation 6; reactant **9**, conformation 3; e. g. Figure 4b) or form a van der Waals complex (e. g. Figure 4c). In the latter case, however, the complex is not parallel to the C_α–C_β bond; such a conformation is less accessible from an *anti* than from a gauche conformation. Particularly interesting is that, for **3**, an *anti*

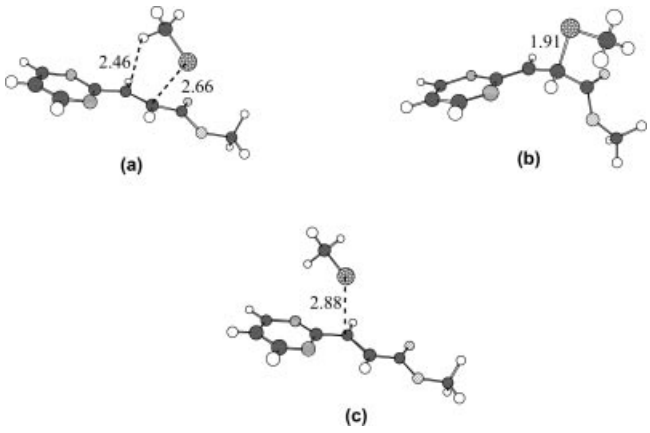

Figure 4. Optimized structures for methanethiolate reaction with **9** in the gas phase: conformations 1 (a), 3 (b), and 6 (c) (see Table 5). Selected distances are in Å. Element patterns are defined in Figure 1.

conformation retains an S–C_β bond (conformation 6) but not an S–C_α bond (conformation 3); while for **9**, an S–C_α but not an S–C_β bond is retained. This suggests again that **3** prefers nucleophilic addition at the β-carbon atom, while **9** prefers addition at the α-carbon atom.

The exception to these trends is that gauche conformation 2 for reactant **9** retains the S–C_α bond upon optimization, rather than forming a van der Waals complex. Note, however, that the S–C_α distance is longer in this case (1.98 Å) than in the other two structures that retain the S–C_α or S–C_β bond (1.91 and 1.93 Å), suggesting that the tendency to form a van der Waals complex with the methanethiolate parallel to the C_α–C_β bond is in competition with the tendency to retain the S–C_α bond.

These considerations lead to the following picture of nucleophilic addition by methanethiolate. When a methanethiolate approaches C_α of **3** or C_β of **9**, a van der Waals complex is favored and reaction is unlikely. When a methanethiolate approaches C_β of **3** or C_α of **9**, a van der Waals complex is favored if the approach is from a gauche direction, but if the approach is from an *anti* direction or possibly from directly over the carbon atom, an S–C bond may form, giving a species with a sufficiently long lifetime for protonation to occur and yield a stable product.

In summary, both the constrained energetics and the unconstrained structures suggest the same regioselectivity for methanethiolate as for cyanide anion addition. The stabilities of the structures will of course be sensitive to solvation, just as the relative energies of α- and β-transition states are sensitive to solvation for the cyanide anion. A full assessment of all factors for methanethiolate attack would be a separate and significant undertaking. Furthermore, while electronic factors should be very similar for methane- and propanethiolate, the possibility that steric factors render the regioselectivies subtly different needs to be considered. However, the results presented here strongly suggest that the regioselectivities for nucleophilic attack of cyanide anion and of propanethiolate on compounds **2**, **3**, **9**, and **10** are similar, as might be expected on the basis of the nucleophiles' similar degrees of softness.

Conclusions

We have shown that nucleophilic attack on an α,β-unsaturated carbonyl compound can be redirected from the usual β-addition (Michael addition) to α-addition by attaching a substituent with a π-deficient aromatic ring to the β-carbon atom. In particular, propanethiolate addition to **2** and **9** results in the usual formation of the β-carbon adduct, while the addition to the stronger π-deficient *N*-oxide **10** occurs at the α-carbon atom and addition to **3** gives a mixture of α- and β-carbon adducts. The Hammett constants σ^- are predictive of the regioselectivity. Density functional calculations using cyanide anion or methanethiolate as the nucleophile reveal that the regioselectivity is due to both a decrease in the transition-state energy for α-attack and increases in the transition-state energies for β- and carbonyl-attack as the aromatic ring is made more π-deficient. The calculations also suggest a significant solvent contribution to the regioselectivity, particularly for compounds such as **3** and **9**, for which the transition states for α- and β-addition have similar gas-phase energies.

Experimental Section

General: ^{1}H (400 MHz) and ^{13}C (100 MHz) NMR spectra were determined for solutions in $CHCl_3$. Mass spectra (MS and HR-MS) were obtained with electron impact (EI, 20 eV). Elemental analyses were determined at the Microanalytical Laboratory of the Adam Mickiewicz University in Poznan, Poland. Merck Kieselgel 60-F_{254} sheets were used for TLC and products were detected with 254-nm light. Merck Kieselgel 60 (230–400 mesh) was used for column chromatography.

Ethyl (*E*)-3-(Pyridin-3-yl)propenoate (2): To a stirred solution of 3-pyridinylcarbaldehyde (**1**, 0.107 g, 1 mmol) in anhydrous CH_3CN (6 mL) (ethoxycarbonylmethylene)triphenylphosphorane (0.329 g, 1.1 mmol) was added in one portion. The resulting solution was stirred at ambient temperature overnight and then concentrated. The residue was column-chromatographed ($CHCl_3$ → 2% MeOH/$CHCl_3$) to give **2** (0.17 g, 96%) as an oil. IR ($CHCl_3$): $\tilde{\nu}$ = 1708, 1622 w cm^{-1}. ^{1}H NMR: δ = 1.35 (t, J = 7.1 Hz, 3 H), 4.29 (q, J = 7.1 Hz, 2 H), 6.93 (d, J = 15.0 Hz, 1 H), 7.28 (ddd, J = 1.0, 4.8, 5.8 Hz, 1 H), 7.45 (d, J = 7.8 Hz, 1 H), 7.73 (d, J = 15.0 Hz, 1 H), 7.78 (td, J = 1.8, 7.7 Hz, 1 H), 8.67 (dd, J = 0.7, 4.7 Hz, 1 H) ppm. ^{13}C NMR: δ = 14.7, 61.1, 122.6, 124.5, 124.6, 137.2, 143.7, 150.5, 153.4, 167.2 ppm. MS (EI): m/z = 177 (15) [M^+], 132 (100) [M^+ – 45]. $C_{10}H_{11}NO_2$ (177.20): calcd. C 67.78, H 6.26, N 7.90; found C 67.27, H 6.57, N 7.65.

Ethyl (*E*)-3-(1-Oxidopyridin-3-yl)propenoate (3). Procedure A: *m*CPBA (70%) (0.153 g, 0.62 mmol) was added in one portion to a stirred solution of **2** (0.10 g, 0.56 mmol) in CH_2Cl_2 (5 mL), and the resulting solution was stirred at ambient temperature overnight. Then the mixture was partitioned ($NaHCO_3$/H_2O/CH_2Cl_2) and the organic phase was washed (brine), dried ($MgSO_4$) and the solvents were evaporated. Column chromatography (EtOAc/hexane, 30 → 70%) gave **3** (0.10 g, 92%) as a solidified oil. IR ($CHCl_3$): $\tilde{\nu}$ = 1710 cm^{-1}. ^{1}H NMR: δ = 1.34 (t, J = 7.1 Hz, 3 H), 4.28 (q, J =

7.1 Hz, 2 H), 7.01 (d, J = 16.2 Hz, 1 H), 7.24–7.29 (m, 2 H, collapsed with solvent), 7.54–7.57 (m, 1 H), 8.01 (d, J = 16.2 Hz, 1 H), 8.27–8.29 (m, 1 H) ppm. ^{13}C NMR: δ = 14.6, 61.4, 125.3, 125.4, 125.8, 126.1, 126.2, 134.3, 140.9, 145.7, 166.7 ppm. MS (EI): m/z = 193 (10) [M^+], 148 (20) [M^+ – 45] 120 (80) [M^+ – 73], 92 (100) [M^+ – 101]. $C_{10}H_{11}NO_3$ (193.20): calcd. C 62.17, H 5.74, N 7.25; found C 62.57, H 5.37, N 7.62.

Ethyl 3-Propylthio-3-(pyridin-3-yl)propenoate (4). Procedure B: Propanethiol (0.13 mL, 112 mg, 1.47 mmol) was added to a stirred solution of EtONa in EtOH [prepared from Na (30 mg, 1.30 mmol) and EtOH (2 mL)] at ambient temperature. After 15 min, a solution of **2** (65 mg, 0.37 mmol) in EtOH (4 mL) was added, and the mixture was allowed to stand for 24 h. The resulting mixture was concentrated to dryness under vacuum and the residue was partitioned $CHCl_3/H_2O$. The organic layer was washed with H_2O (5 mL), dried ($MgSO_4$), concentrated and column-chromatographed ($CHCl_3$ → 1% MeOH) to give **4** (68 mg, 73%) as a yellow oil. IR ($CHCl_3$): $\tilde{\nu}$ = 1725 cm^{-1}. ^{1}H NMR: δ = 0.90 (t, J = 7.3 Hz, 3 H), 1.17 (t, J = 7.1 Hz, 3 H), 1.50 (sept, J = 7.3 Hz, 2 H), 2.40 (t, J = 7.3 Hz, 3 H), 2.92 (dd, J = 16.2, 6.7 Hz, 1 H), 3.20 (dd, J = 16.2, 8.6 Hz, 1 H), 4.08 (dq, J = 11.5, 7.2 Hz, 2 H), 4.36 (dd, J = 8.5, 6.7 Hz, 1 H), 7.14 (ddd, J = 5.8, 4.9, 1.1 Hz, 1 H), 7.35 (d, J = 7.8 Hz, 1 H), 7.64 (td, J = 7.7, 1.8 Hz, 1 H), 8.53 (dd, J = 4.8, 0.8 Hz, 1 H) ppm. ^{13}C NMR: δ = 13.8, 14.5, 23.1, 33.2, 39.8, 46.5, 61.0, 122.5, 123.1, 136.9, 149.6, 161.1, 171.6 ppm. HRMS (EI): m/z = 253.1142 (10) [M^+]; calcd. for $C_{13}H_{19}NO_2S$ 253.1136.

Ethyl 3-Propylthio-3-(1-oxidopyridin-3-yl)propenoate (5) and Ethyl 2-propylthio-3-(1-oxidopyridin-3-yl)propenoate (6): Treatment of **3** (40 mg, 0.21 mmol) with propanethiol (0.07 mL, 64 mg, 0.84 mmol) by procedure B [column chromatography ($CHCl_3$ → 2% MeOH/$CHCl_3$)] gave **5** and **6** [38 mg, 68%; as an inseparable mixture of β (**5**) and α (**6**) adduct in a 1:2 ratio as estimated on the basis of the ^{1}H NMR spectrum] as an oil. IR ($CHCl_3$): $\tilde{\nu}$ = 1723 cm^{-1}. ^{1}H NMR: δ = 0.92 (t, J = 7.3 Hz, 3 H from β, and 3 H from α), 1.21 (t, J = 7.1 Hz, 3 H from β), 1.24 (t, J = 7.1 Hz, 3 H from α), 1.59 (sept, J = 7.3 Hz, 2 H from α), 1.62 (sept, J = 7.3 Hz, 2 H from β), 2.49–2.56 (m, 2 H, SCH_2 from β), 2.58–2.71 (m, 2 H, SCH_2 from α), 2.96 (dd, J = 16.2, 7.6 Hz, 1 H from β), 3.12 (dd, J = 16.2, 6.7 Hz, 1 H from β), 3.26 (dd, J = 13.7, 7.3 Hz, 1 H from α), 3.42 (dd, J = 13.7, 7.9 Hz, 1 H from α), 4.09–4.19 (m, 2 H from α, 2 H from β and 1 H from α), 4.99 (t, J = 7.15 Hz, 1 H from β), 7.15–7.22 (m, 2 H_{Ar} from α, and 2 H_{Ar} from β), 7.31–7.35 (m, 1 H_{Ar} from α), 7.64 (dd, J = 2.8, 7.9 Hz, 1 H_{Ar} from β), 8.17–8.24 (m, 1 H_{Ar} from α, and 1 H_{Ar} from β) ppm. ^{13}C NMR: δ = 13.7 (CH_3 α),13.8 (CH_3 β), 14.5, 23.0 (CH_2 α), 23.1 (CH_2 β), 30.1, 34.4, 35.2 38.5, 40.1, 42.3, 61.2, 61.7, 124.5, 124.9, 125.7, 125.9, 126.0, 128.4, 140.0, 140.1, 148.7, 152.2 170.8, 172.7 ppm. HRMS (EI): m/z = 269.1092 (25) [M^+]; calcd. for $C_{13}H_{19}NO_3S$ 269.1086.

Methyl Pyrimidine-2-carboxylate (7): 2-Cyanopyrimidine[20] (420 mg, 4.0 mmol) was dissolved in methanol (20 mL), saturated with HCl, and the resulting mixture was heated to reflux for 2 h. The volatiles were evaporated to dryness under vacuum and the residue was partitioned with $CHCl_3/H_2O$. The organic layer was washed ($NaHCO_3$, H_2O, brine), dried ($MgSO_4$) and the solvents were evaporated. Column chromatography ($CHCl_3$ → 4% MeOH/$CHCl_3$) gave (350 mg, 80%) of the desired compound:[21] ^{1}H NMR: δ = 4.11 (s, 3 H), 7.53 (t, J = 4.9 Hz, 1 H), 8.98 (d, J = 4.9 Hz, 2 H) ppm. ^{13}C NMR: δ = 54.1, 123.6, 156.8, 158.4, 164.1 ppm.

Ethyl (*E*)-3-(Pyrimidin-2-yl)propenoate (9): DIBAL/hexane (0.1 M; 0.13 mL, 0.73 mmol) was added over 20 min to a stirred solution of methyl pyrimidine-2-carboxylate (**7**, 0.10 g, 0.73 mmol) in CH_2Cl_2 (10 mL) at –70 °C (dry ice/acetone). After 1 h, no starting material was detected by TLC ($CHCl_3$/MeOH, 9:1; R_f = 0.75). To this solution, still kept at –70 °C, (ethoxycarbonylmethylene)triphenylphosphorane (0.27 g, 0.79 mmol) was added and the mixture was allowed to warm to room temp. over 1 h. The reaction was quenched with satd. aq. NH_4Cl (6 mL) and the organic phase was washed (brine), dried ($MgSO_4$) and the solvents were evaporated. Column chromatography (EtOAc/hexane, 20 → 50%) gave **9** (58 mg, 48%) as an oil. IR ($CHCl_3$): $\tilde{\nu}$ = 1716, 1648 w cm^{-1}. ^{1}H NMR: δ = 1.34 (t, J = 7.1 Hz, 3 H), 4.28 (q, J = 7.1 Hz, 2 H), 7.20 (d, J = 15.8 Hz, 1 H), 7.23 (t, J = 4.9 Hz, 1 H), 7.70 (d, J = 15.8 Hz, 1 H), 8.78 (d, J = 4.7 Hz, 2 H). ^{13}C NMR: δ = 14.6, 61.3, 120.6, 127.9, 143.1, 157.6, 163.4, 166.6 ppm. MS (EI): m/z = 178 (20) [M^+], 133 (100) [M^+ – 45]. $C_9H_{10}N_2O_2$ (178.19): calcd. C 60.66, H 5.66, N 15.72; found C 60.37, H 5.57, N 15.65.

Ethyl (*E*)-3-(1-Oxidopyrimidin-2-yl)propenoate (10): Treatment of **9** (85 mg, 0.48 mmol) with *m*CPBA (70%; 0.13 g, 0.53 mmol) according to procedure A [column chromatography ($CHCl_3$ → 5% MeOH/$CHCl_3$)] gave **10** (52 mg, 56%) and starting material **9** (15 mg). IR ($CHCl_3$): $\tilde{\nu}$ = 1717 cm^{-1}. ^{1}H NMR: δ = 1.34 (t, J = 7.1 Hz, 3 H), 4.30 (q, J = 7.1 Hz, 2 H), 7.24 (t, J = 4.5 Hz, 1 H), 7.30 (d, J = 15.8 Hz, 1 H), 8.26 (d, J = 15.8 Hz, 1 H), 8.28 (dd, J = 1.4, 4.1 Hz, 1 H), 8.42 (dd, J = 1.5, 6.6 Hz, 1 H) ppm. ^{13}C NMR: δ = 14.6, 61.5, 121.2, 130.1, 132.1, 144.0, 146.1, 155.6, 166.2 ppm. MS (EI): m/z = 194 (8) [M^+], 149 (20) [M^+ – 45] 121 (100) [M^+ – 73]. $C_9H_{10}N_2O_3$ (194.19): calcd. C 55.67, H 5.19, N 14.43; found C 55.37, H 5.37, N 14.65.

Ethyl 3-Propylthio-3-(pyrimidin-2-yl)propenoate (11): Treatment of **9** (44 mg, 0.25 mmol) with propanethiol (0.09 mL, 76 mg, 1.0 mmol) according to procedure B [column chromatography ($CHCl_3$)] gave **11** (42 mg, 67%) as an oil. IR ($CHCl_3$): $\tilde{\nu}$ = 1729 cm^{-1}. ^{1}H NMR: δ = 0.91 (t, J = 7.3 Hz, 3 H), 1.15(t, J = 7.16 Hz, 3 H), 1.54 (sept, J = 7.3 Hz, 2 H), 2.53 (m, J = 7.3 Hz, 2 H), 2.96 (dd, J = 16.5, 6.0 Hz, 1 H), 3.20 (dd, J = 16.5, 9.6 Hz, 1 H), 4.08 (qt, J = 7.14, 3.6 Hz 2 H), 4.45 (dd, J = 9.6, 6.0 Hz, 1 H), 7.15 (t, J = 4.9 Hz, 1 H), 8.67 (d, J = 4.9 Hz, 1 H) ppm. ^{13}C NMR: δ = 13.8, 14.5, 23.2, 33.4, 38.7, 46.9, 61.0, 119.5, 157.6, 170.7, 171.5 ppm. HRMS (EI): m/z = 254.1103 (10) [M^+]; calcd. for $C_{12}H_{18}N_2O_2S$ 254.1089.

Ethyl 2-Propylthio-3-(1-oxidopyrimidin-2-yl)propenoate (12): Treatment of **4** (26 mg, 0.134 mmol) with propanethiol (0.05 mL, 41 mg, 0.54 mmol) according to procedure B [column chromatography ($CHCl_3$ → 2% MeOH/$CHCl_3$)] gave **12** (24 mg, 67%) as an oil. IR ($CHCl_3$): $\tilde{\nu}$ = 1730 cm^{-1}. ^{1}H NMR: δ = 0.98 (t, J = 7.3 Hz, 3 H), 1.26 (t, J = 7.2 Hz, 3 H), 1.64 (sept, J = 7.3 Hz, 2 H), 2.71 (m, J = 7.3 Hz, 2 H), 3.51 (dd, J = 17.8, 5.7 Hz, 1 H), 3.70 (dd, J = 17.8, 9.7 Hz, 1 H), 4.02 (dd, J = 9.7, 5.7 Hz, 1 H), 4.42 (q, J = 7.2 Hz, 2 H) 7.23 (dd, J = 6.3, 4.9 Hz, 1 H), 8.18 (dd, J = 4.7, 1.2 Hz, 1 H), 8.40 (dd, J = 6.5, 1.3 Hz, 1 H) ppm. ^{13}C NMR: δ = 13.8, 14.6, 22.9, 33.7, 34.5, 42.0, 61.6, 119.9, 143.1, 144.8, 160.1, 172.2 ppm. HRMS (EI): m/z = 270.1030 (27) [M]$^+$; calcd. for $C_{12}H_{18}N_2O_3S$ 270.1038.

Computational Methods: Fully optimized reactants and transition states were computed in the gas phase for each model compound at the B3LYP/6-31+G(d)[22–25] level using the software packages Gaussian98 and Gaussian03.[26] The level of theory was chosen on the basis of previous work in which the α- and β-addition of cyanide anion to a set of 22 α,β-unsaturated carbonyl compounds yielded average differences of 2 kcal/mol between HF/6-31+G(d) and B3LYP/6-31+G(d) energies for reactants and transition states.[12] Energy differences at these levels of theory also compared well to previously published MP2 values. Frequency calculations were performed to verify the nature of all stationary points, transi-

tion states having one imaginary frequency. Van der Waals complexes for cyanide anion addition were computed by beginning with transition state structures and optimizing. Starting from α- and carbonyl-transition states generally led to the same van der Waals complex, with the cyanide anion above the plane of the larger molecule and roughly 3 Å from the carbonyl carbon atom. Starting from the β-transition states always led to van der Waals complexes of lower energy in which all heavy atoms were in the same plane, and the cyanide anion was roughly 3 Å from the ring on the opposite side of the α,β-unsaturated carbonyl moiety. The low-energy van der Waals complexes are shown in Figure 5. The transition state energies in Table 1 are the barrier heights relative to the lowest-energy van der Waals complex in all cases; these van der Waals complexes are shown in Figure 5. The low-energy van der Waals complexes were all stable by more than 12 kcal/mol relative to isolated reactants, so entropic contributions are unlikely to destabilize them. For consistency, the same van der Waals complex was used as the reference for all additions to a given substrate. These give only a qualitative idea of the actual barrier heights, as an accurate calculation would require a full conformational search for van der Waals complexes and a more accurate method than B3LYP, which performs well for transition states but poorly for van der Waals complexes.[14] This was adequate for our purposes, though, since the relative rather than the absolute barrier heights are critical for predicting the regioselectivity. Transition-state free energies, $G^{\ddagger}$, were computed at 298 K in the usual manner from the harmonic frequencies and the rigid rotor moments of inertia and are represented by $\Delta G^{\ddagger}$ [i.e., relative to the $G^{\ddagger}_{\beta}$ for the β-transition state as per Equation (1)] in Table 2. The energies of the B3LYP-optimized transition states were also calculated at the MP2/6-31+G(d) level for comparison. These were combined with enthalpy and entropy corrections for 298 K from the B3LYP results to yield the MP2 values of $\Delta G^{\ddagger}$ in Table 2. Partial atomic charges for **2**, **3**, **9**, and **10** were calculated from the B3LYP/6-31+G(d) electron density using the ChelpG method. Atomic orbital coefficients for the LUMO of **2**, **3**, **9**, and **10** were calculated at the B3LYP/6-31G level for the B3LYP/6-31+G(d)-optimized geometries. The charges and atomic-orbital coefficients are given in Table 4. Free energies of solvation (ΔG_{solv}) were calculated at the gas-phase-optimized geometries using the PCM continuum solvation method[18,19] with a dielectric constant of 7.58, representative of THF, at the HF/6-31+G(d) level of theory. A Table of ΔG_{solv} can be found in the Supporting Information (see also the footnote on the first page of this article).

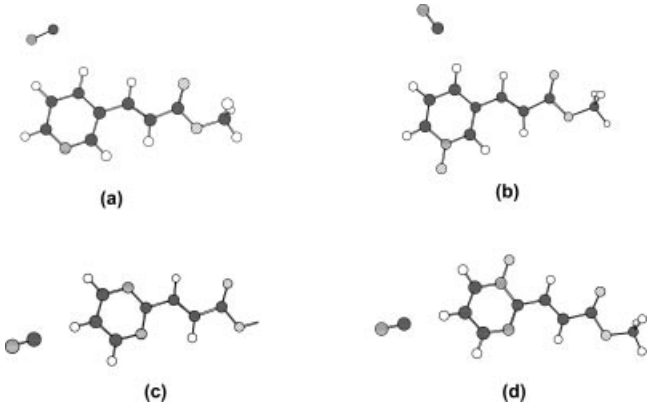

Figure 5. Van der Waals complexes of cyanide anion and (a) **2**, (b) **3**, (c) **9**, and (d) **10** [B3LYP/6-31+G(d)].

[1] E. D. Bergman, D. Ginsburg, R. Pappo, *Org. React.* **1959**, *10*, 179–555.
[2] E. Lewandowska, S. Kinastowski, S. F. Wnuk, *Can. J. Chem.* **2002**, *80*, 192–199.
[3] I. V. Solodin, A. V. Eremeev, I. I. Chervin, R. G. Kostayanovskii, *Kim. Geterotsikl. Soedin.* **1985**, 1359–1362.
[4] B. M. Trost, J. L. Gunzner, T. Yasukata, *Tetrahedron Lett.* **2001**, *42*, 3775–3778.
[5] J. G. Shim, J. C. Park, C. S. Cho, S. C. Shim, Y. Yamamoto, *Chem. Commun.* **2002**, 852–853.
[6] B. M. Trost, G. R. Dake, *J. Am. Chem. Soc.* **1997**, *119*, 7595–7596.
[7] B. Liu, R. Davis, B. Joshi, D. W. Reynolds, *J. Org. Chem.* **2002**, *67*, 4595–4598.
[8] A. Kamimura, N. Murakami, K. Yokota, M. Shirai, H. Okamoto, *Tetrahedron Lett.* **2002**, *43*, 7521–7523.
[9] A. Kamimura, N. Murakami, F. Kawahara, K. Yokota, Y. Omata, K. Matsuura, Y. Oishi, R. Morita, H. Mitsudera, H. Suzukawa, A. Kakehi, M. Shirai, H. Okamoto, *Tetrahedron* **2003**, *59*, 9537–9546.
[10] M. J. Aurell, M. J. Banuls, R. Mestres, E. Munoz, *Tetrahedron* **1999**, *55*, 831–846.
[11] M. J. Aurell, M. J. Banuls, R. Mestres, E. Munoz, *Tetrahedron* **2001**, *57*, 1067–1074.
[12] D. C. Chatfield, A. Augsten, C. D′Cunha, E. Lewandowska, S. F. Wnuk, *Euro. J. Org. Chem.* **2004**, 313–322.
[13] O. Miyata, T. Shinada, I. Ninomiya, T. Naito, T. Date, K. Okamura, S. Inagaki, *J. Org. Chem.* **1991**, *56*, 6556–6564.
[14] C. J. Cramer, *Essentials of Computational Chemistry*, John Wiley & Sons, Chichester, England, **2002**.
[15] G. S. Hammond, *J. Am. Chem. Soc.* **1955**, *77*, 334–338.
[16] L. E. Chirlian, M. M. Francl, *J. Comput. Chem.* **1987**, *8*, 894–904.
[17] I. Fleming, *Frontier Orbitals and Organic Chemical Reactions*, John Wiley & Sons, New York, **1976**.
[18] S. Miertus, E. Scrocco, J. Tomasi, *Chem. Phys.* **1981**, *55*, 117–129.
[19] S. Miertus, J. Tomasi, *Chem. Phys.* **1982**, *65*, 239–245.
[20] K. Hermann, G. Simchen, *Liebigs Ann. Chem.* **1981**, 333–341.
[21] W. P. Mamaev, E. A. Graczeva, *Kim. Geterotsikl. Soedin.* **1969**, 1086–1088.
[22] A. D. Becke, *J. Chem. Phys.* **1992**, *96*, 2155–2160.
[23] A. D. Becke, *J. Chem. Phys.* **1992**, *97*, 9173–9177.
[24] A. D. Becke, *J. Chem. Phys.* **1993**, *98*, 5648–5652.
[25] C. T. Lee, W. T. Yang, R. G. Parr, *Phys. Rev. B* **1988**, *37*, 785–789.
[26] J. J. Frisch, G. W. Trucks, H. B. Schlegel, G. E. Scuseria, M. A. Robb, J. R. Cheeseman, V. G. Zakrzewski, J. A. Montgomer, R. E. Stratmann, J. C. Burant, S. Dapprich, J. M. Millam, A. D. Daniels, K. N. Kudin, M. C. Strain, O. Farkas, J. Tomasi, V. Barone, M. Cossi, R. Cammi, B. Mennucci, C. Polmelli, C. Adamo, S. Clifford, J. Ochterski, G. A. Petersson, P. Y. Ayala, Q. Cui, K. Morokuma, D. K. Malick, A. D. Rabuck, K. Raghavachar, J. B. Foresman, J. Cioslowski, J. V. Ortiz, B. B. Stefanov, A. L. G. Lui, P. Piskorz, I. Komaromi, R. Gomperts, R. L. Martin, D. J. Fox, T. Keith, M. A. Al-Laham, C. Y. Peng, A. Nanayakkara, C. Gonzlez, M. Challacombe, P. M. W. Gill, B. G. Johnson, W. Chen, M. W. Wong, J. L. Andres, M. Head-Gordon, E. S. Replogle, J. A. Pople, *Gaussian 03, Revision C.02*, Gaussian, Inc., Wallingford, CT, **2004**.
[27] C. Hansch, A. Leo, D. Hoekman, *Exploring QSAR: Hydrophobic, Electronic, and Steric Constants*, American Chemical Society, Washington, DC, **1995**.

Received: January 24, 2005

